PHYSICAL REVIEW C **87**, 051304(R) (2013)

Decay pattern of the pygmy dipole resonance in ^{60}Ni

M. Scheck,[1,*] V. Yu. Ponomarev,[1] T. Aumann,[1] J. Beller,[1] M. Fritzsche,[1,†] J. Isaak,[1,2,3] J. H. Kelley,[4,5] E. Kwan,[5,6,‡] N. Pietralla,[1] R. Raut,[5,6,§] C. Romig,[1] G. Rusev,[5,6,‖] D. Savran,[2,3] K. Sonnabend,[3] A. P. Tonchev,[5,‡] W. Tornow,[5,6] H. R. Weller,[5,6] and M. Zweidinger[1]

[1]*Institut für Kernphysik, Technische Universität Darmstadt, D-64289 Darmstadt, Germany*
[2]*ExtreMe Matter Institute EMMI and Research Division GSI Helmholtzzentrum für Schwerionenforschung GmbH, D-64291 Darmstadt, Germany*
[3]*Institut für Angewandte Physik, Goethe-Universität Frankfurt, D-60438 Frankfurt a.M., Germany*
[4]*Department of Physics, North Carolina State University, Raleigh, North Carolina 27695, USA*
[5]*Triangle Universities Nuclear Laboratory, Durham, North Carolina 27708, USA*
[6]*Department of Physics, Duke University, Durham, North Carolina 27708, USA*

(Received 4 January 2013; revised manuscript received 13 March 2013; published 15 May 2013)

Spin-1 states in ^{60}Ni were excited with the $(\vec{\gamma},\gamma')$ reaction, exploiting the High Intensity $\vec{\gamma}$-ray Source at Triangle University Nuclear Laboratory. This facility is capable of providing fully linearly polarized, quasimonochromatic, Compton-backscattered photons in the entrance channel of the reaction. The depopulation of low-lying levels in an energy region far below the incident quasimonochromatic photons allows us to obtain average branching ratios of the excited spin-1 states. Levels within the energy region associated with the PDR showed regular behavior and ≈75% of their decays are direct ground-state decays. The levels in the energy region above the PDR exhibit a statistical decay behavior to a large number of low-lying excited states and have only ≈50–60% branches to the ground state. Within the framework of the quasiparticle phonon model this feature can be explained with the number of quasiparticles contributing to the wave functions of the excited spin-1 states. Quasimonochromatic photon beams provide a new method to test the microscopic nature of 1^- levels.

DOI: 10.1103/PhysRevC.87.051304 PACS number(s): 23.20.Lv, 21.60.Jz, 25.20.Dc, 27.50.+e

During recent decades a great deal of attention has been paid to the dipole response of the nucleus. Of particular interest and currently heavily debated [1,2] is the pygmy dipole resonance (PDR) [3,4], which is within a geometrical picture visualized as the vibration of a neutron skin versus an isospin saturated $N = Z$ core. The PDR is in stable nuclei experimentally recognized as an accumulation of $J^\pi = 1^-$ states carrying extra $E1$ strength in the energy region between 5 and 9 MeV [5–7]. An energy region that is well below the giant dipole resonance (GDR) [8], whose maximum is located near 15 MeV for medium mass nuclei. The latter is in a geometrical picture associated with vibration of all protons versus all neutrons. While the GDR exhausts almost 100% of the $E1$ strength predicted by the Thomas-Reiche-Kuhn sum rule, the PDR exhausts only a few percent. Furthermore, the GDR has a large spreading width of several MeV. As consequence, the tail of the GDR still reaches into the energy region where the PDR is located. Hence, the observed 1^- levels cannot be easily attributed to one of the two resonances.

One of the groundbreaking approaches revealing the internal structure of levels associated with either of the two modes was the comparison of $(\alpha,\alpha'\gamma)$ experiments and (γ,γ') photon-scattering experiments [9,10]. While the photons excite all spin-1 levels independently of their isoscalar or isovector nature, the isoscalar α particle is very sensitive to spin-1 states with an isoscalar nature, as is expected for the PDR. In contrast, the GDR is an isovector excitation. The comparison revealed that only the lower part of the accumulated 1^- levels is a surface mode with strong isoscalar components.

In nuclei the decay pattern of excited states below the neutron separation threshold may provide complementary information on the wave functions of these states. While the states are excited predominantly via 1p1h (one-particle one-hole) or two-quasiparticle (QP) components of their wave functions, they may decay to intermediate-energy states from NpNh components as well. Individual $J^\pi = 1^-$ states associated with the GDR have a very small fraction of 1p1h components and the density of nearby intermediate states is very high. Altogether, for the γ-decay channel this leads to a statistical decay of the GDR via cascades. The contribution of 1p1h components to the wave functions of the PDR states is much larger. This results in a large branching ratio to the ground state, usually assumed to be 100%. The associated matrix elements for the transitions to the ground state in the PDR region can be inferred by exploring the nuclear resonance fluoresence (NRF) technique [11]. Recently, the cascade decays from the high-energy part of the PDR have been observed in ^{138}Ba$(\vec{\gamma},\gamma')$ [12] and ^{142}Nd$(\vec{\gamma},\gamma')$ [13] experiments. Hence, it is natural to expect direct decays of the PDR levels to the low-lying excited states as precursors of the cascades.

A perfect tool to study dipole excitations in nuclei is the NRF technique. Since photons are massless, the angular

*mscheck@ikp.tu-darmstadt.de
†Present address: Areva NP GmbH, D-91052 Erlangen, Germany.
‡Present address: Physics Division, Lawrence Livermore National Laboratory, Livermore, California 94551, USA.
§Present address: UGC-DAE Consortium for Scientific Research, Kolkata Centre, Kolkata 700098, India.
‖Present address: Chemistry Division, Los Alamos National Laboratory, Los Alamos, New Mexico 87545, USA.

momentum transfer in the (γ, γ') reaction is almost entirely limited to their intrinsic angular momentum of $1\,\hbar$. However, the scattering of real photons goes hand in hand with a large background from photons scattered nonresonantly in the atomic system. Therefore, in conventional NRF experiments employing bremsstrahlung in the entrance channel, transitions in the low-energy region have a low peak-to-background ratio or are even below the sensitivity limit. Furthermore, decay branches are often too weak to be observed. Even if such decays are observed it is not a simple task to separate decays to the ground state from the ones to excited states. It is done by combining experiments with different endpoint energies and applying the Ritz variational principle (e.g., see Ref. [14]).

We employ a different technique and report in this publication the unambiguous measurement of the branching ratios to several low-lying states from the PDR states in ^{60}Ni. The use of a monochromatic beam results in less background in the low-energy region. Thus, even if the decay branch from one individual photoexcited state to a lower-lying level is below the sensitivity limit, it is still possible to measure the accumulated feeding of several decay branches to the level under investigation by observing the depopulation of the low-lying level. A (γ, γ') experiment in which energy regions are scanned systematically [15] and ground-state decays, as well as decays from lower-lying levels, can be measured simultaneously will reveal at least an average branching ratio for the levels situated in the energy region covered by the incident photon beam.

The experiments were performed at the High Intensity $\vec{\gamma}$-ray Source (HI$\vec{\gamma}$S) operated by Triangle University Nuclear Laboratory (TUNL) [16]. A wiggler in a free electron laser (FEL) is used to stimulate electrons, confined as two electron bunches in a storage ring, to emit light in the electron volt range. The laser light is reflected in a mirror system and then Compton backscattered from the second circulating electron bunch. The Compton-backscattering process boosts the energies of the scattered photons in the MeV range but also conserves the well-defined transversal polarization of the FEL photons. Using a lead collimator installed in the beam tube, only a small angular range of the Compton backscattered γ rays is accepted at the scattering probe of interest. This procedure results in quasimonochromatic, fully linearly polarized photon beams in the entrance channel of the $(\vec{\gamma}, \gamma')$ reaction. The Compton-backscattered photon beam was collimated with $1''$ in diameter lead collimator. The diameter of this collimator and its distance to the collision point (60 m) defines the width ($\pm 3\%$ of the mean photon energy) of the Gaussian-shaped spectral distribution of the photon flux. In total seven ranges with mean energies between 7.65 and 9.66 MeV were measured.

The detector setup consisted of four high-purity germanium (HPGe) detectors. Each detector had an intrinsic efficiency of 60% relative to the $3'' \times 3''$ NaI standard. The detectors were placed in a crosslike, close geometry around the ^{60}Ni target at polar angles of $\theta = 90^\circ$ with respect to the incident photon beam. Two detectors were placed in the polarization plane (PP) at azimuthal angles of $\phi = 0^\circ$ and 180°, and two detectors were perpendicular to the PP ($\phi = 90^\circ$ and 270°), respectively. The PP is defined by the γ ray's direction of motion and the

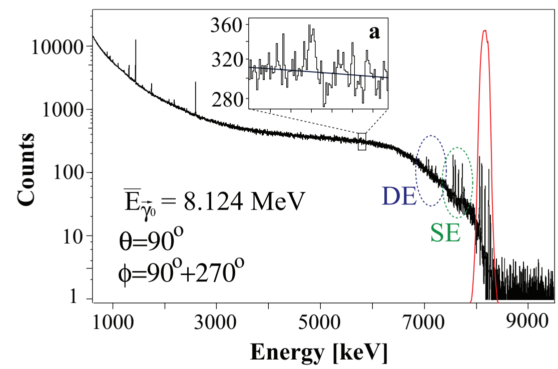

FIG. 1. (Color online) A spectrum recorded perpendicular to the polarization plane. The mean energy of the incident photon beam was $\bar{E}_{\gamma_0} = 8.124$ MeV. The inset (a) shows a peak at 5800.2 keV belonging to a transition of a $J^\pi = 1^-$ level at 8086 keV to the first excited 0^+ state at 2285 keV. The straight red line indicates the spectral distribution of the incident photon beam. Labels denote the energy regions, where single-escape peaks (SE) and double-escape peaks (DE) are found.

transversal polarization vector. The target consisted of 2.996 g of ^{60}Ni enriched to 99.8%. Up to 3.5 MeV efficiency calibration of the horizontal and vertical detectors was obtained using standard γ-ray sources. The detector response up to 10 MeV was simulated using GEANT4 [17]. In the source calibration a horizontal versus vertical asymmetry of approximately 5% was observed. This asymmetry was reproduced when calculating the effective angular distributions, $W(\theta, \phi)$, following the formalism outlined in Ref. [18] and considering the geometry realized in the experiment.

Fully polarized photons in the entrance channel are used to determine the parity of a spin-1 state. This is feasable, as for a $J^\pi = 1^+(1^-)$ state the elastic scattering process of excitation from and decay to the ground state happens almost entirely within (perpendicular to) the PP. However, in this work the quasimonochromacy of the incident photon beam at HI$\vec{\gamma}$S is exploited. A typical spectrum recorded perpendicular to the PP at a mean photon energy of $\bar{E}_{\gamma_0} = 8.124$ MeV is shown in Fig. 1. In the region covered by the incident photon beam, a number of peaks belonging to ground-state transitions of 1^- levels are clearly visible. Furthermore, Fig. 1(a) shows a peak belonging to the decay of a $J^\pi = 1^-$ level at 8086 keV to the first excited 0^+ state at 2285 keV. In the low-energy region the background is due to atomic Compton scattering in the target sample. In the high-energy region it is dominated by events for which at least one γ ray in the detection cascade escaped from the finite volume of the detector.

The $M1$- and $E1$-strength distributions, taking into account firmly assigned decays to lower-lying states, are shown in Figs. 2(a) and 2(b). Therein, for better comparison the reduced ground-state decay widths, $\Gamma_0^{\rm red} = \Gamma_0/E^3$, are plotted. These are directly propotional to the respective $B(\Pi1)\uparrow$ excitation probability [11]. The $\Pi1$ strengths ($\Pi = E$ or M) were extracted in a series of (γ, γ') experiments using unpolarized bremsstrahlung in the entrance channel [19]. The $M1$-strength distribution exhibits the typical pattern of the isoscalar and isovector spin-flip $M1$ resonances [20]. The

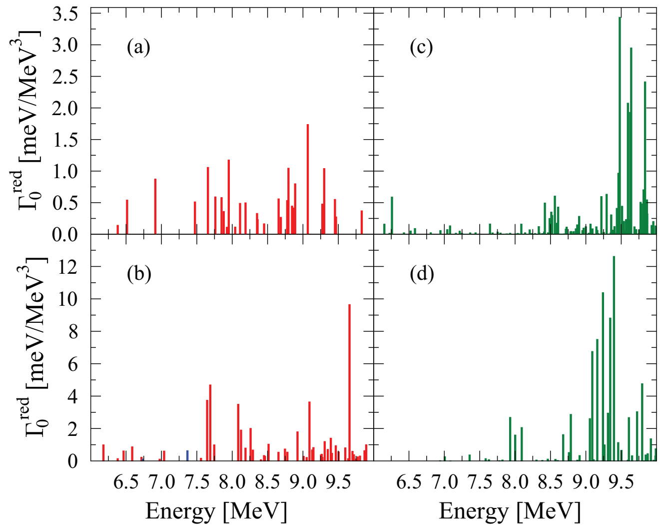

FIG. 2. (Color online) Left-hand side: Partial experimental (red [gray]) $M1$- (a) and $E1$- (b) strength distributions of ^{60}Ni in the investigated energy region. Levels (blue [gray] bars) for which no parity could be assigned are attributed to the $E1$-strength distribution. Right-hand side: Theoretical (green [gray]) $M1$- (c) and $E1$- (d) strength distribution calculated within the QPM. The experimental strength distributions were extracted from a combination of this work and a bremstrahlungs measurement [19]. In the strength distributions only firmly assigned transitions to lower-lying states were considered. Please note the different scaling on the y axis.

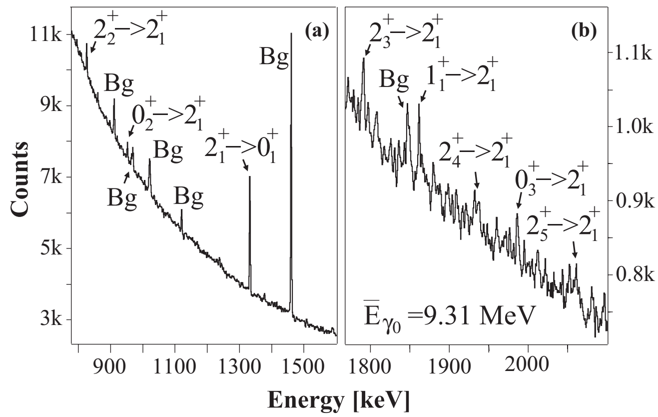

FIG. 3. Parts of a spectrum recorded perpendicular to the polarization plane. The mean energy of the incident photon beam was $\bar{E}_{\gamma_0} = 9.31$ MeV. Peaks belonging to transitions depopulating low-lying excited states of ^{60}Ni are labeled. Furthermore, peaks stemming from background transitions are labeled as BG. Please note the different scaling of the y axis.

summed $M1$ strength for the two $M1$ resonances accumulates to a total of $B(M1)\uparrow = 3.94(28)\mu_N^2$. An excitation strength in good agreement with the values usually measured in the $A \approx 60$ mass region, e.g., in ^{56}Fe the $B(M1)\uparrow$ strength for the $M1$ resonances, was determined to 3.83(18) μ_N^2 [21]. In the $E1$-strength distribution a local accumulation of stronger excited $J^\pi = 1^-$ levels appears near 8-MeV excitation energy.

Figures 2(c) and 2(d) present the reduced ground-state decay widths, Γ_0^{red}, calculated within the quasiparticle phonon model (QPM) [22] for magnetic and electric dipole states, respectively. The obtained fragmentation of the strength is the result of coupling one-phonon $1^\pm$ states, which carry the main part of the decaying strength to two- and three-phonon configurations. The latter configurations with energies below 15 MeV are made up of phonons with multipolarity from $0^\pm$ to $8^\pm$. The microscopic structure of these phonons was calculated exploiting the random phase approximation. The calculation predicted a reasonable amount of the strength located at a slightly higher energy in comparison to the data. Similar results were reported for ^{58}Ni in Ref. [14].

In Fig. 3 two low-energy regions of the spectrum recorded perpendicular to the PP with a mean beam energy $\bar{E}_{\gamma_0} = 9310$ keV are illustrated. Clearly, several peaks corresponding to transitions depopulating low-lying excited states of ^{60}Ni [23] are present. As the sensitivity limit for a peak to be accounted as such, three standard deviations of the underlying background were used.

As pointed out earlier, the decays to low-lying states of levels populated by the primary γ-ray transitions are often too weak to be accounted as peaks in the spectra, but in the low-lying level the feeding of several such transitions can accumulate to a decent population. Therefore, the depopulation of the low-lying level yields information about the summed feeding from spin-1 states in the energy range covered by the incident photon beam. In Ref. [12] it was possible from the observed horizontal-vertical assymmetry to conclude that the population happened by negative-parity spin-1 states. However, as many of the transitions depopulating the fed low-lying levels are weak and the stronger depopulating levels receive additional feeding from levels just above, the errors of the asymmetry are too large to allow for any conclusive assignment. A strong argument that the vast majority of the population of the low-lying levels stems from the negative-parity spin-1 states is the strength of the $M1$ resonances as extracted from the bremsstrahlung experiments [19]. There, except for two weakly excited levels for the $J^\pi = 1^+$ states, no branchings to any lower-lying state were observed. In NRF experiments the measured integrated cross section, $I_{s,f}$, for a given decay channel f is proportional to the product of the ground-state decay width Γ_0 and the branching ratio, Γ_f/Γ, of the partial decay width Γ_f and total decay width $\Gamma = \sum_f \Gamma_f$. Therefore, the attribution of a larger fraction of the observed inelastic decays to the levels forming the $M1$ resonances would increase their strength to an insensate $M1$-excitation strength. Furthermore, in the ^{56}Fe bremsstrahlung NRF measurement (see Sec. IVc in Ref. [14]) a certain but not drastic amount of feeding was observed. In the recent publication reporting on an experiment using quasimonochromatic, linearly polarized photons [21], no decays from lower-lying states were reported. Furthermore, the QPM calculations indicate that the $M1$-strength-generating spin-flip excitations in ^{56}Fe and ^{60}Ni are similar. Hence the $M1$ resonances can be expected to exhibit a strong resemblance. Consequently, it can be concluded that at least the major fraction of the intensity of the depopulation of the low-lying states stems from feeding by 1^- levels.

In the low-energy part of the spectra only transitions from levels with spin and parity $J^\pi = 0^+, 1^+, 2^+$ were observed. An observation, that is, in accordance with previous observations for ^{58}Ni [14] and for one spin-1 level in ^{62}Ni [24]. In none of these three isotopes was the depopulation of low-lying 3^+ and 4^+ levels observed. This experimental finding indicates that the population of the low-lying levels happens directly via dipole transitions from the photoexcited spin-1 levels and no further intermediate levels are involved. By exploiting the quasimonochromacy of the incident γ-ray beam, it is possible to address average feeding of lower-lying states and, consequently, decay branchings of the primarily excited spin-1 states to specific energy regions. Therefore, the observed peak areas were corrected for efficiency and angular distribution. Furthermore, the observed feeding from other low-lying levels was included. The errors for the efficiency were assumed to be 10% in the high-energy region and 5% in the low-energy region, which is almost entirely covered by the source calibration. For the ground-state branchings, the angular distributions are calculated in a straightforward manner, while the angular distributions of the observed depopulating transitions from the low-lying levels are sensitive toward the population history of these levels. They depend on the fraction of feeding from other low-lying levels and whether the direct population stems from 1^+ or 1^- levels. To account in the analysis for the uncertainty of the parity of the feeding spin-1 level, the angular distributions of the depopulating decays were weighted with the intensity fraction observed for the ground-state decays of the excited spin-1 levels and the observed population by the feeding from other low-lying levels. The corresponding error was estimated to be 10%. The results are presented in Table I and illustrated in Fig. 4.

In the energy region where the $E1$-strength distribution [Fig. 2(b)] exhibits several strongly excited 1^- levels ($\bar{E}_{\gamma_0} =$ 7650 and 8124 keV) the ground-state decays exhaust about 70–80% of the total intensity. Excluding levels for which the branching was observed directly, as for example for the strongly excited level at 8086 keV (see Fig. 1, $\Gamma_{2_1^+}/\Gamma_{\rm tot} = 0.06(2)$ and $\Gamma_{0_2^+}/\Gamma_{\rm tot} = 0.13(4)$ [19]), does not change the average ground-state branching ratio. This branching ratio drops above the PDR region, indicating a change of the structure of the excited spin-1 levels. For the energy region covered with the highest photon-beam energy used in this work, an even more drastic change is recognizable when the strongly excited level at 9659 keV and its observed branching to the first excited 2_1^+ level [$\Gamma_{2_1^+}/\Gamma_{\rm tot} = 0.10(3)$] are excluded.

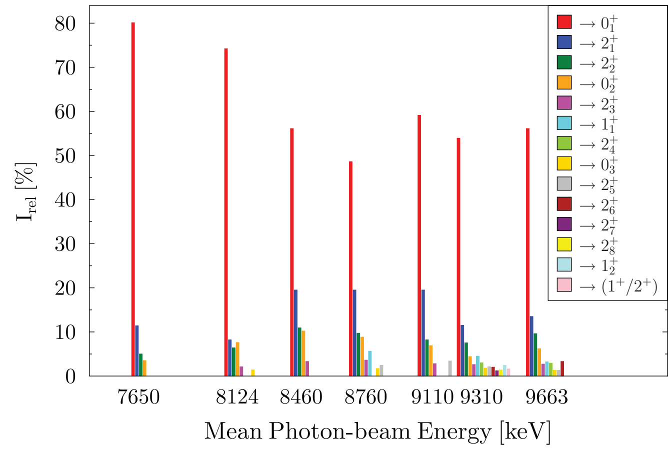

FIG. 4. (Color online) Observed relative intensities, $I_{\rm rel}$, for the decays of the spin-1 states to the given final levels. The values represent an average of all $J = 1$ levels in the respective energy range covered by the incident photon beam. A detailed discussion is given in the text and the values are presented in Table I.

TABLE I. Number of 1^- $N(1^-)$ and 1^+ $N(1^+)$ states, the ratio of the ground-state intensities (R), and the relative branching ratios ($\Gamma_f/\Gamma_{\rm tot}$) to the final states for each energy region measured.

		7650	8124	8460	8760	9110	9310	9663
$N(1^-)/N(1^+)$		4/2	5/8	9/7	5/7	15/10	18/10	10/2
$R = \frac{I_{0,1^-}}{I_{0,1^+}}$		7.0(16)	5.2(6)	3.0(5)	1.4(2)	2.3(3)	1.3(2)	41(12)
E_f (keV)	J_f^π	$\Gamma_f/\Gamma_{\rm tot}$ (%)	$\Gamma_f/\Gamma_{\rm tot}$ (%)	$\Gamma_f/\Gamma_{\rm tot}$ (%)	$\Gamma_f/\Gamma_{\rm tot}$ (%)	$\Gamma_f/\Gamma_{\rm tot}$ (%)	$\Gamma_f/\Gamma_{\rm tot}$ (%)	$\Gamma_f/\Gamma_{\rm tot}$ (%)
0	0^+	80.1(70)	74.2(57)	56.1(81)	48.6(73)	59.1(66)	53.9(69)	56.1(67)
1332.5	2^+	11.4(60)	8.2(32)	19.5(72)	19.5(65)	19.5(59)	11.5(40)	13.5(44)
2158.6	2^+	5.0(35)	6.4(29)	10.9(49)	9.7(36)	8.2(27)	7.5(37)	9.6(31)
2284.9	0^+	3.5(26)	7.6(34)	10.2(52)	8.8(41)	6.9(29)	4.4(22)	6.2(25)
3124.0	2^+		2.1(15)	3.3(26)	3.6(28)	2.8(18)	2.6(17)	2.7(17)
3194.0	1^+				5.6(32)		4.5(22)	3.2(25)
3269.4	2^+						3.0(22)	2.9(24)
3318.7	0^+		1.4(7)		1.7(15)		1.8(11)	1.3(9)
3393.5	2^+				2.4(20)	3.4(22)	2.1(16)	1.3(12)
3736.3	2^+						2.0(17)	3.3(24)
3887.8	2^+						1.2(10)	
4007.9	2^+						1.4(14)	
4020.5	1^+						2.4(16)	
4319.0	$1^+, 2^+$						1.6(14)	

In this case the elastic scattering for the other levels in this region corresponds to only 27(10)%.

Besides the change in the average branching behavior, an increase in the number of fed low-lying states with the mean energy of the incident photon beam is obvious. The latter supports a more complex structure of the excited spin-1 levels, which opens more decay channels to lower-lying states with a similar structure.

These observations are in accordance with the microscopic picture for 1^- levels as drawn by the QPM. The PDR levels exhibit rather low inelastic branchings and the final levels are the fundamental building blocks of vibrational structures, such as the one-phonon 2^+_1 or two-phonon states (2^+_2 and 0^+_2). The PDR states are excited via one-phonon 1^-_i components of their wave functions while the decay to low-lying λ^π_k states takes place from complex $[1^-_i \otimes \lambda^\pi_k]_{1^-}$ components. With increasing excitation energy the states have a stronger admixture of complex components and exhibit larger inelastic branchings, with often higher-lying excited levels as final states.

In this work it has been demonstrated that the decay behavior of photoexcited spin-1 levels provides useful information about the internal structure of their wave function. Therefore, the exploitation of quasimonochromatic photon beams in the entrance channel of the (γ, γ') reaction provides a powerful experimental approach. The latter will become a versatile tool with the Extreme Light Infrastructure–Nuclear Physics Facility (ELI-NP) [25]. At ELI-NP the high intensity (10^{13} γ/s) and narrow bandwidth (0.1% at 19 MeV) of the incident photon beams will enable the study of the decay behavior of individually resolved levels.

The authors are indebted to the H$\vec{\gamma}$GS facility staff for the excellent photon beams. Furthermore, we thank U. Kneissl for valuable discussions. Financial support by the DFG under Grants No. SFB634, No. Pi393/2-1, and No. SO907/1-2 and the US DOE Grants No. DE-FG02-97ER41033, No. DE-FG02-97ER41042, and No. DE-FG02-97ER41041 is gratefully acknowledged. D. Savran acknowledges support by the Helmholtz Alliance Program of the Helmholtz Association (HA216/EMMI).

[1] P.-G. Reinhard and W. Nazarewicz, Phys. Rev. C **81**, 051303 (2010).
[2] J. Piekarewicz, Phys. Rev. C **83**, 034319 (2011).
[3] G. A. Bartholomew *et al.*, Adv. Nucl. Phys. **7**, 229 (1973).
[4] A. Zilges *et al.*, Phys. Lett. B **542**, 43 (2002).
[5] R.-D. Herzberg *et al.*, Phys. Rev. C **60**, 051307 (1999).
[6] S. Volz *et al.*, Nucl. Phys. A **779**, 1 (2006).
[7] U. Kneissl, N. Pietralla, and A. Zilges, J. Phys. G **32**, R217 (2006).
[8] M. N. Harakeh and A. van der Woude, *Giant Resonances* (Oxford University Press, Oxford, 2001).
[9] D. Savran *et al.*, Phys. Rev. Lett. **97**, 172502 (2006).
[10] J. Endres *et al.*, Phys. Rev. Lett. **105**, 212503 (2010).
[11] U. Kneissl, H. H. Pitz, and A. Zilges, Prog. Part. Nucl. Phys. **37**, 349 (1996).
[12] A. P. Tonchev *et al.*, Conference Proceedings: Symposium on Capture γ-ray Spectroscopy and Related Topics XIV (World Scientific, Singapore, in press).
[13] C. T. Angell *et al.*, Phys. Rev. C **86**, 051302(R) (2012).
[14] F. Bauwens *et al.*, Phys. Rev. C **62**, 024302 (2000).
[15] A. P. Tonchev *et al.*, Phys. Rev. Lett. **104**, 072501 (2010).
[16] H. R. Weller *et al.*, Prog. Part. Nucl. Phys. **62**, 257 (2009).
[17] S. Agostinelli *et al.*, Nucl. Instrum. Methods A **506**, 250 (2003).
[18] L. W. Fagg and S. S. Hanna, Rev. Mod. Phys. **31**, 711 (1959).
[19] M. Scheck *et al.* (in preparation).
[20] K. Heyde, A. Richter, and P. von Neumann Cosel, Rev. Mod. Phys. **82**, 2365 (2010).
[21] T. Shizuma *et al.*, Phys. Rev. C **87**, 024301 (2013).
[22] V. G. Soloviev, *Theory of Atomic Nuclei, Quasiparticles, and Phonons* (IOP, London, 1992).
[23] http://www.nndc.bnl.gov/ensdf/.
[24] R. Moreh *et al.*, Nucl. Phys. A **224**, 86 (1979).
[25] http://www.eli-np.ro/.